

Online Convex Optimization with Binary Constraints

Antoine Lesage-Landry, *Member, IEEE*, Joshua A. Taylor, *Member, IEEE*,
and Duncan S. Callaway, *Member, IEEE*

Abstract— We consider online optimization with binary decision variables and convex loss functions. We design a new algorithm, binary online gradient descent (bOGD), and bound its expected dynamic regret. The bound is sublinear in time and linear in the cumulative variation of the relaxed, continuous round optima. We apply bOGD to demand response with thermostatically controlled loads, in which binary constraints model discrete on/off settings. We also model uncertainty and varying load availability, which depend on temperature deadbands, lock-out of cooling units and manual overrides. We test the performance of bOGD in several simulations based on demand response.

Index Terms— binary decision, demand response, dynamic regret, online convex optimization, thermostatically controlled loads

I. INTRODUCTION

IN online convex optimization (OCO), one makes a decision in each time step to minimize a round-dependent loss function [1], [2]. The loss function is only observed by the decision-maker following the round. These observations are then used to update the decision. The simplicity and computational efficiency of OCO make it well-suited to online applications like demand response in electric power systems [3], [4].

Demand response (DR) with thermostatically controlled loads (TCLs), e.g., residential households [5], [6] or commercial buildings [7], can provide fast timescale services such as frequency regulation and load following [8]. These services can economically improve the operation of power systems [9].

In this work, we formulate an algorithm for online convex optimization with binary constraints, which we refer to as the binary online gradient descent (bOGD). We use bOGD for setpoint tracking with TCLs with discrete on/off settings and lockout constraints, as well as the standard deadband temperature constraint. The lock-out constraint ensures that, after being turned off, a 5-minute period must pass before a cooling unit can be turned on again. Lock-out is a significant

This work was funded by the Natural Sciences and Engineering Research Council of Canada, by the National Science Foundation, award 1351900, and by the Advanced Research Projects Agency-Energy, award DE-AR0001061.

A. Lesage-Landry and D.S. Callaway are with the Energy & Resources Group, University of California, Berkeley, CA, USA {alesagelandry, dcal}@berkeley.edu.

J.A. Taylor is with The Edward S. Rogers Sr. Department of Electrical & Computer Engineering, University of Toronto, Toronto, Ontario, Canada, M5S 3G4. e-mail: josh.taylor@utoronto.ca.

physical limitation of TCLs for fast DR applications, and is rarely accounted for in the literature.

Several decision-making and resource allocation problems have binary constraints, e.g., scheduling [10] or turning off or on a residential load's cooling unit for demand response [5], [6]. In this work, we focus on functions which, without the binary constraint, are convex over the set $[0, 1]^n$, $n \in \mathbb{N}$. In our work, we show that bOGD, an OCO algorithm with an additional randomization step, provides sequential binary decisions with a provable performance guarantee. We show that bOGD has an expected dynamic regret bound that is sublinear in the number of rounds and linear in the cumulative variation between relaxed, continuous round optima. If the cumulative variation is sublinear, then the average expected regret over time goes to zero as the time horizon increases and, therefore, bOGD provides decisions that are, on average, optimal in expectation.

Related work: bOGD is based on OCO [1], [2]. In online optimization, the closest work to ours is [11]. In this work, the authors consider binary decision variables for submodular loss functions and provide a static regret analysis. Several extensions of this work have been proposed, e.g., [12], [13]. Similarly to convexity in continuous optimization, in discrete/combinatorial optimization, submodularity usually implies that a problem can be solved efficiently [14]. Submodular minimization problems can be solved efficiently using either combinatorial algorithms [15] or convex optimization algorithms via the Lovász extension, a continuous and convex extension of the submodular function [14], [16]. In our work, we minimize convex functions over the binary set $\{0, 1\}^n$, where convexity is over the continuous set $[0, 1]^n$. Convexity over the continuous set does not imply submodularity over the binary set, and nor does submodularity imply convexity. Consider, for example, a twice differentiable function $f : [0, 1]^n \mapsto \mathbb{R}$. Then, f is submodular if all of its mixed second-order derivatives are nonpositive [14], whereas f is convex over $[0, 1]^n$ if the Hessian is positive semi-definite. While both conditions can be met simultaneously, neither of them implies the other.

The loss function of the this work's motivating application, setpoint tracking with TCLs, is convex but not submodular, and thus falls outside the scope of [11]. We also provide a stronger performance guarantee than [11] by showing that bOGD has a bounded dynamic regret bound.

Randomized expert and bandit-based algorithms have also been developed for online problems with binary decision

variables [11], [17]. In the general case, these algorithms are computationally inefficient due to the large number of possible experts or decisions, 2^n [11]. Several efficient algorithms for binary decisions have been proposed in online linear optimization [18] (and the references therein) under restrictive assumptions, e.g., a constant total number of 1-decisions being selected and linear loss functions.

Binary constraints were considered in the context of time-varying optimization of power systems in [19]–[21]. In [19], a similar randomization step is used to accommodate loads with discrete settings. The performance of the randomization step is, however, only characterized through an asymptotic bound on the dual variables of the problem. Reference [20] also models discrete decisions and lock-out using the approach of [21]. In [21], the authors extend the error diffusion algorithm. In each round, the decision is given by the projection onto the discrete set of the cumulative difference between the continuous (relaxed) and the discrete decisions. An example of demand response with heaters that includes binary decisions and lock-out constraints is provided. The performance analysis of [20] and [21] ensures that the cumulative difference between the continuous and discrete decisions is bounded, but it does not characterize the difference between the round optimum and the discrete decision made in each round.

In this work, our specific contributions are:

- We handle binary constraints in OCO using a randomization step. To the best of our knowledge, binary decision variables have not previously been integrated into OCO.
- We obtain an expected dynamic regret bound for the resulting algorithm, bOGD , that is sublinear in time and linear in the cumulative variation of relaxed round optima.
- We use bOGD for DR with TCLs with binary on/off settings. We also account for the unavailability of loads for DR caused by temperature deadbands, lock-out constraints, and manual override.

The remainder of the paper is organized as follows. We formulate the basic problem in Section II and analyze the regret of bOGD in Section III. We apply bOGD to demand response with TCLs in Section IV. The algorithm's performance is numerically evaluated in Section IV-B. We conclude in Section V.

II. OCO WITH BINARY CONSTRAINTS

We denote the round by t and the time horizon by τ . Let $\hat{\mathbf{x}}_t \in \{0, 1\}^n$ and $\mathbf{x}_t \in [0, 1]^n$ be, respectively, the discrete decision and the relaxed, continuous decision variables at round t . Let $f_t : [0, 1]^n \mapsto \mathbb{R}^n$, $n \in \mathbb{N}$, be the differentiable loss function at round t for $t = 1, 2, \dots, \tau$. We assume that f_t is convex and bounded over $[0, 1]^n$. The convexity of f_t and compactness of the relaxed domain imply that f_t is Lipschitz continuous with respect to a norm $\|\cdot\|$ [22] for all $\mathbf{x} \in [0, 1]^n$ and $t = 1, 2, \dots, \tau$. Let $L_1, L_2 \in (0, +\infty)$ be the Lipschitz continuity modulus with respect to the ℓ_1 - and ℓ_2 -norm, respectively. Thus, $\|\nabla f_t(\mathbf{x})\|_1 \leq L_1$ and $\|\nabla f_t(\mathbf{x})\|_2 \leq L_2$ for all t and $\mathbf{x} \in [0, 1]^n$ and all t .

The binary-constrained OCO problem is as follows. In each

round t , the decision-maker must solve:

$$\min_{\hat{\mathbf{x}}_t \in \{0, 1\}^n} f_t(\hat{\mathbf{x}}_t), \quad (1)$$

where f_t is only known after round t . The performance of OCO algorithms are evaluated in terms of the regret [1], [2], [23]. In this work, we use the dynamic regret [23], [24], which represents the cumulative loss difference between the actual decision and the round optimum computed in hindsight. In this case, the dynamic regret takes the following form:

$$R_\tau = \sum_{t=1}^{\tau} f_t(\hat{\mathbf{x}}_t) - f_t(\mathbf{b}_t^*),$$

where $\hat{\mathbf{x}}_t$ is the decision at t and $\mathbf{b}_t^* \in \arg \min_{\mathbf{x} \in \{0, 1\}^n} f_t(\mathbf{x})$, the round optimum. Because we use an additional randomization step to deal with the binary nature of the decision variable, we bound the expectation of the dynamic regret. We seek an algorithm with a sublinear bound [1], [2], which implies that $\mathbb{E}[R_\tau]/\tau \rightarrow 0$ as $\tau \rightarrow +\infty$. Finally, it is common to bound the dynamic regret as a function of the cumulative variation in the relaxed round optima, V_τ [23], [24]. This term characterizes how much the sequence of relaxed optima changes through time. Let $V_\tau = \sum_{t=1}^{\tau} \|\mathbf{x}_{t+1}^* - \mathbf{x}_t^*\|_2$ where $\mathbf{x}_t^* \in \arg \min_{\mathbf{x} \in [0, 1]^n} f_t(\mathbf{x})$. We use the bOGD update to solve (1), given by

$$\mathbf{x}_{t+1} = \arg \min_{\mathbf{x} \in [0, 1]^n} \eta \nabla f_t(\mathbf{x}_t)^\top \mathbf{x} + \frac{1}{2} \|\mathbf{x} - \mathbf{x}_t\|_2^2 + \eta \lambda \|\mathbf{x}\|_1 \quad (2)$$

$$\hat{\mathbf{x}}_{t+1} = \mathcal{R}(\mathbf{x}_{t+1}), \quad (3)$$

where $\lambda \geq 0$ controls the optional ℓ_1 -regularizer, $\eta \geq 0$ is the descent step size to be set shortly, and $\mathcal{R} : [0, 1]^n \mapsto \{0, 1\}^n$ is a the randomization function. The function \mathcal{R} returns a 0–1 vector where each entry i is sampled from a Bernoulli random variable with probability $p = \mathbf{x}_t(i)$. We note that $\mathbb{E}[\hat{\mathbf{x}}_t] \equiv \mathbb{E}[\mathcal{R}(\mathbf{x}_t)] = \mathbf{x}_t$.

For example, in the context of DR with TCLs, update (2)–(3) provides, first, the relaxed, continuous decision to solve the problem at time t . Second, the randomization step converts the continuous decision to the appropriate binary control. In this case, $\hat{\mathbf{x}}_t(i) = 1$ and $\hat{\mathbf{x}}_t(i) = 0$ represents, respectively, turning on or off load i 's cooling unit.

III. REGRET ANALYSIS

We now present two intermediate results that will be used to derive bOGD 's dynamic regret bound. We first show that the expected difference between the loss associated with the randomized binary and the relaxed decisions is bounded above for all rounds.

Lemma 1: Let the binary decision variable $\hat{\mathbf{x}}_t$ be computed using bOGD . If $\eta \geq \frac{1}{L_1}$, then

$$\mathbb{E}[|f_t(\hat{\mathbf{x}}_t) - f_t(\mathbf{x}_t)|] \leq \eta L_1 L_2 \sqrt{n+1}.$$

The proof of Lemma 1 is provided in Appendix A. Using Lemma 1, we can provide a sublinear regret bound for bOGD when it is used over the constrained time horizon $T \leq \tau$. The constrained time horizon T is based on the Lipschitz continuity

modulus with respect to the 1-norm and the step size, a . It can therefore be computed before implementation.

Lemma 2: Suppose $T \leq (aL_1)^2$, $a > 0$, and set $\eta = \frac{a}{\sqrt{T}}$. The expect regret of bOGD is upper bounded by

$$\mathbb{E} [R_T] \leq \left(\frac{n}{2a} + \frac{a(L_2)^2}{2} + aL_1L_2\sqrt{n+1} \right) \sqrt{T} + 2nL_1V_T.$$

The proof of this lemma is presented in Appendix B. Lemma 2 means that if V_T is sublinear, the worst-case performance of the decision-maker will improve over time for $t \leq T$. We use Lemma 2 to obtain the following regret bound for any time horizon, τ .

Theorem 1 (Regret bound for bOGD): Let $T \leq (aL_1)^2$ and $a > 0$. Suppose bOGD with $\eta = \frac{a}{\sqrt{T}}$ is reinitialized every T rounds. Then, the expected cumulative regret over the time horizon τ is bounded above by:

$$\mathbb{E} [R_\tau] \leq \left(\frac{n}{2a} + \frac{3aL_2^2}{2} + aL_1L_2\sqrt{n+1} \right) \tau^\epsilon + 2nL_1V_\tau,$$

where $0 < \epsilon < 1$. Consequently, $\mathbb{E} [R_\tau]$ is sublinear if $V_\tau < O(\tau)$.

Proof: Suppose that the algorithm is restarted after $T \leq (aL_1)^2$ rounds and reinitialized. Let $m \in \mathbb{N}$ denote the number of times the algorithm has been restarted. Let $N = \tau/T$ be the number of times the algorithm is required to be restarted throughout the time horizon τ . We assume that $N \in \mathbb{N}$, rounding up τ/T if it is not integer.

Let $R_{t_0:t_1} = \sum_{t=t_0}^{t_1} f_t(\hat{\mathbf{x}}_t) - f_t(\mathbf{b}_t^*)$ be the cumulative regret from round t_0 to t_1 . By Lemma 2, we have,

$$\mathbb{E} [R_{mT+1:(m+1)T}] \leq c_1 \sqrt{(m+1)T - mT} + c_2 V_{mT+1:(m+1)T},$$

where $c_1 = \frac{n}{2a} + \frac{a(L_2)^2}{2} + aL_1L_2\sqrt{n+1}$, $c_2 = 2nL_1$, and $V_{t_0:t_1} = \sum_{t=t_0}^{t_1} \|\mathbf{x}_{t+1}^* - \mathbf{x}_t^*\|$. Then, the cumulative regret is

$$\begin{aligned} \mathbb{E} [R_\tau] &= \sum_{m=1}^N \mathbb{E} [R_{mT+1:(m+1)T}] \\ &\leq \sum_{m=1}^N c_1 T^{\frac{1}{2}} + c_2 \sum_{m=1}^N V_{mT+1:(m+1)T} \\ &= c_1 NT^{\frac{1}{2}} + c_2 V_\tau. \end{aligned} \quad (4)$$

By definition, $\tau = NT$, thus there exists $\epsilon \in (0, 1)$ such that $\tau^\epsilon \geq NT^{\frac{1}{2}}$. We rewrite (4) as

$$\mathbb{E} [R_\tau] \leq c_1 \tau^\epsilon + c_2 V_\tau,$$

which completes the proof. \blacksquare

Supposing $V_\tau < O(\tau)$, Theorem 1 implies that the regret is sublinear and $\mathbb{E} [R_\tau]/\tau$ goes to zero as the time horizon τ increases. bOGD can accommodate V_τ that is almost linear whereas standard OCO algorithms [23], [24] are limited to $V_\tau < O(\sqrt{\tau})$.

The proposed bound is looser than prevalent dynamic OCO algorithms [23]–[25] because of the τ^ϵ term. If, for example, $\tau = 10^4$ and setting $T = 100$, the regret is bounded by

$O(\tau^{\frac{3}{4}} + V_\tau)$. The difference in the regret bound order in τ is explained in part by the randomization step used to deal with the binary constraints. The randomization adds an extra term to the regret of standard continuous-variable OGD-based algorithms, as shown in (12) from Appendix B. This term increases the order of the regret bound because of the multiple restarts.

IV. APPLICATION TO DEMAND RESPONSE

We use bOGD for setpoint tracking with thermostatically controlled loads. We present next the setpoint tracking setup and then evaluate its performance in numerical simulations.

A. Setup

We consider n TCLs. The load parameters are:

- $\mathbf{r} \in \mathbb{R}_+^n$, where $\mathbf{r}(i)$ is the thermal resistance of load i ;
- $\mathbf{c} \in \mathbb{R}_+^n$, where $\mathbf{c}(i)$ is the thermal capacitance of load i ;
- $\boldsymbol{\theta}_d \in \mathbb{R}^n$, where $\boldsymbol{\theta}_d(i)$ is load i 's desired temperature;
- $\bar{\boldsymbol{\theta}}, \underline{\boldsymbol{\theta}} \in \mathbb{R}^n$, where $\bar{\boldsymbol{\theta}}(i)$ and $\underline{\boldsymbol{\theta}}(i)$ are respectively the maximum and minimum temperature of load i 's temperature deadband.

The load parameters are assumed to be known. The below online parameters are observed at the end of each round:

- $s_t \in \mathbb{R}$, the power setpoint to track;
- $\tilde{\mathbf{p}}_t \in \mathbb{R}_+^n$, where $\tilde{\mathbf{p}}_t(i)$ is the power consumption at time t of load i 's cooling unit when it is not available for DR because it is constrained by its temperature, lock-out or manual override;
- $\mathbf{p}_t \in \mathbb{R}_+^n$, where $\mathbf{p}_t(i)$ represents the power consumption of load i and time t when it is controllable, i.e., when it is not constrained by the deadband, lock-out, or by the manual override.
- $\boldsymbol{\theta}_t \in \mathbb{R}^n$, where $\boldsymbol{\theta}_t(i)$ is the indoor temperature at time t of load i . Let $\langle \boldsymbol{\theta} \rangle_t \in \mathbb{R}^n$ be the vector of temperatures averaged over rounds 1 to t ;
- $\theta_t^{\text{ambient}} \in \mathbb{R}$ is the ambient (outdoor) temperature. The ambient temperature is the same for all loads. This assumption simplifies the computation but can be relaxed;
- $\mathbf{u}_t \in \{0, 1\}^n$ is the cooling unit override at time t of load i . When $\mathbf{u}_t(i) = 1$, the local cooling unit overrides the DR control because the temperature is above the deadband. It also represents rounds when the user manually controls the cooling unit, which we model as uncertain.

We note that the online parameters represent observations or measurements.

Lastly, let $\hat{\mathbf{x}}_t(i) = 1$ and $\hat{\mathbf{x}}_t(i) = 0$ be, respectively, the signal to turn on and off load i 's cooling unit.

The model and update rule are given in Algorithm 1. We use (5) from [4] as the loss function. In (5), $\rho > 0$ and $\lambda > 0$ are numerical parameters. There are three terms, as explained below.

- 1) *Setpoint tracking losses.* This term is used to match the total power consumption of the loads to the regulation signal, s_t . The power consumption of the TCLs is split into two components: the controllable part dispatched by

$$\begin{aligned}
f_t(\hat{\mathbf{x}}_t) = & (s_t - \mathbf{p}_t^\top \hat{\mathbf{x}}_t - \tilde{\mathbf{p}}_t^\top \mathbf{u}_t)^2 + \lambda \|\hat{\mathbf{x}}_t\|_1 \\
& + \frac{\rho}{2} \left\| \frac{t-1}{t} \langle \boldsymbol{\theta} \rangle_{t-1} + \frac{1}{t} \left(\mathbf{B} \boldsymbol{\theta}_{t-1} + (\mathbf{I} - \mathbf{B}) (\mathbf{1} \theta_t^{\text{ambient}} - \hat{\mathbf{x}}_t \text{diag}(\mathbf{r}) \text{diag}(\mathbf{p}_t)) \right) - \boldsymbol{\theta}_d \right\|_2^2
\end{aligned} \tag{5}$$

Algorithm 1 bOGD for setpoint tracking with TCLs

Parameters: T, a, ρ, λ, h
Initialization: Set $\mathbf{x}_1 \in [0, 1]^n$, $\eta = \frac{a}{\sqrt{T}}$, and $K = \frac{5}{60h}$

- 1: **for** $t = 1, 2, \dots, T$ **do**
- 2: Implement binary decisions $\hat{\mathbf{x}}_t = \mathcal{R}(\mathbf{x}_t)$.
- 3: Observe all online parameters: $\mathbf{p}_t, \tilde{\mathbf{p}}_t, \mathbf{u}_t, \boldsymbol{\theta}_t, s_t, \theta_t^{\text{ambient}}$.
- 4: Compute the mean temperature $\langle \boldsymbol{\theta} \rangle_{t-1}$.
- 5: Update the relaxed decision variable \mathbf{x}_{t+1} :

$$\mathbf{x}_{t+1} = \arg \min_{\mathbf{x} \in [0, 1]^n} \eta \nabla f_t(\mathbf{x}_t)^\top \mathbf{x} + \frac{1}{2} \|\mathbf{x} - \mathbf{x}_t\|_2^2 + \eta \lambda \|\mathbf{x}\|_1.$$

- 6: **end for**

the algorithm, $\mathbf{p}_t^\top \hat{\mathbf{x}}_t$, and the uncontrollable part, $\tilde{\mathbf{p}}_t^\top \mathbf{u}_t$, set by the loads to meet their constraints. The squared tracking error penalizes large deviations.

- 2) *Sparsity regularizer.* This 1-norm term is used to avoid sending non-zero control signals to loads that are not available at a given round, e.g., if their temperature is out of the deadband or during lock-out. The availability of a load i is expressed by $\mathbf{p}_t(i) \neq 0$. It is also used to minimize the number of loads dispatched and to avoid sending small signals to the loads. The sparsity regularizer is directly incorporated to the update instead of being taken into account via the gradient. This is done to improve the regularization performance [26].
- 3) *Mean temperature regularizer.* This 2-norm term minimizes the long-term impact of demand response on the loads by promoting a small difference between the average and desired temperatures. While the temperatures used in Algorithm 1 are based on measurements, we use the following discrete-time approximation to model the impact of turning on the cooling units on the temperature [5], [27]:

$$\boldsymbol{\theta}_{t+1} = \mathbf{B} \boldsymbol{\theta}_t + (\mathbf{I} - \mathbf{B}) (\mathbf{1} \theta_t^{\text{ambient}} - \hat{\mathbf{x}}_t \text{diag}(\mathbf{r}) \text{diag}(\mathbf{p}_t)), \tag{6}$$

where $\mathbf{1}$ is the n -dimensional vector of ones and $\mathbf{B} = \text{diag} \left(\exp \left(-\frac{h}{\mathbf{r}(i)\mathbf{c}(i)} \right), \text{ for } i = 1, 2, \dots, n \right)$.

The temperature deadband, the lock-out constraints, and the manual override are incorporated into the model via \mathbf{p}_t . The loads measure their power consumption according to their availability and set \mathbf{p}_t locally, which is then observed by the algorithm. A load is available if its temperature is within the deadband, not in lock-out and not manually controlled by the user. The logical rules governing $\mathbf{p}_t(i)$ are summarized below:

- (*deadband*) If $\theta_{t-1}(i) < \underline{\theta}(i)$, then the load sets $\mathbf{p}_t(i) = 0$.
- (*deadband*) If $\theta_{t-1}(i) > \bar{\theta}(i)$, then the load sets $\mathbf{p}_t(i) = 0$. The cooling unit is activated via the override control,

i.e., $\mathbf{u}_t(i) = 1$ and $\tilde{\mathbf{p}}_t(i) \neq 0$.

- (*manual override*) If the load manually uses its cooling unit regardless of deadband constraints and DR, $\mathbf{u}_t(i) = 1$, $\mathbf{p}_t(i) = 0$, and $\tilde{\mathbf{p}}_t(i) \neq 0$.
- (*lock-out*) If $\mathbf{p}_{k-1}(i)\hat{\mathbf{x}}_{k-1}(i) + \tilde{\mathbf{p}}_{k-1}(i)\mathbf{u}_{k-1}(i) > 0$ and $\mathbf{p}_k(i)\hat{\mathbf{x}}_k(i) + \tilde{\mathbf{p}}_k(i)\mathbf{u}_k(i) = 0$ for any $k \in \{t-1, t-2, \dots, t-K\}$ where K is the number of rounds representing a duration of M minutes, then $\mathbf{p}_t(i) = 0$ and $\mathbf{u}_t(i) = 0$. In other words, if the cooling unit was shut down in the past M minutes, then is unavailable for control.
- (*available load*) Otherwise, load i is available and $\mathbf{p}_t(i) \neq 0$.

B. Numerical example

We consider an aggregation of $n = 1000$ TCLs. We assume that the loads have access to two-way communication infrastructure. They can receive cooling instructions and can report their power consumption and temperature to and from the DR aggregator. For example, the different sensors, thermostat and cooling unit's controller, can all be connected using different local communication protocols, e.g. Wi-Fi or ZigBee [28], to a hub which is itself internet-enabled. Information to and from the DR aggregator can then be communicated via the Internet.

All load parameters are sampled uniformly from [27, Table I]. We set the lock-out time M to be 5 minutes. Let $s_t = s_0 + w_t$ be the random and intermittent regulation signals where w_t is constant for 5 rounds and then sampled according to $w_t \sim N(0, 300)$. We set $s_0 = 2400$ kW so that loads can balance maintaining their temperature within their deadband and tracking the setpoints. The initial decision $\mathbf{x}_1(i)$ is set randomly to 0 or 1 with a probability of 0.5 for all $i = 1, 2, \dots, n$.

The ambient temperature for the short time horizon is $\theta_{\text{ambient}}^{\text{ambient}} = \theta_0^{\text{ambient}} + 0.25 \sin(t\pi/T)$ where $\theta_0^{\text{ambient}} = 34^\circ\text{C}$. We let the initial temperature of the TCLs be their desired ones, $\boldsymbol{\theta}_d$. The load temperature evolves as (6) plus zero-mean Gaussian noise with variance 0.025. The regularizer parameters are set to $\sigma = 500$ and $\lambda = 250$, and the step size parameter to $a = 4 \times 10^{-4}$. For the numerical calculations, we use the parser CVXPY [29] with the solver Gurobi [30].

Figure 1 shows bOGD, bOGD without randomization, and the optimal continuous dispatch, each summed up with the uncontrollable part of the TCLs power consumption, the setpoint, and the uncontrollable power consumption presented individually. Figure 1 shows the power consumption of bOGD, of bOGD without randomization, and of the optimal continuous dispatch – all of which include the uncontrollable part of the TCLs power consumption –, the setpoint, and the uncontrollable power consumption presented individually. The uncontrollable power consumption, $\tilde{\mathbf{p}}_t^\top \mathbf{u}_t$, represents all

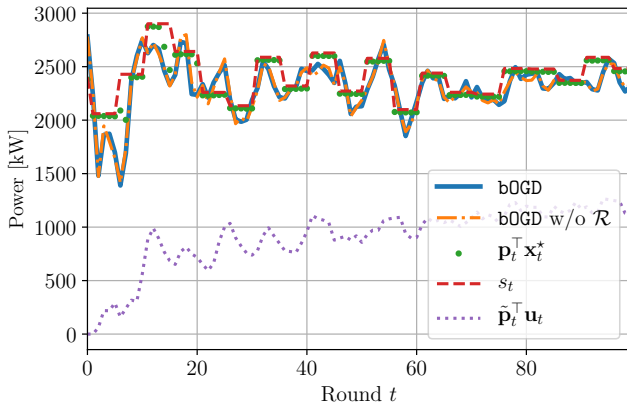


Fig. 1. Demand response performance of bOGD with TCLs

decisions taken locally by the loads to ensure that their temperatures stay within the deadband. The relative difference between the power consumption using randomized decisions and the relaxed, continuous decisions is, on average, 1.34%. The average relative tracking error of the randomized and relaxed decisions are 6.91% and 6.92%, respectively. We note the higher tracking error at the start of the simulation. This is due to the limited number of temperature measurements used by the mean-temperature regularizer in the first rounds. The method requires, on average, 90.2 milliseconds on a 2.4 GHz Intel Core i5 laptop computer to evaluate the DR decisions for $n = 1000$ loads. This illustrates the algorithm's high scalability and the potential for real-time implementation.

Figure 2 shows two temperature profiles observed during the simulation. In Figure 2a, the TCL is dispatched on several occasions, including once over several rounds. Near the end of the simulation, the TCL is constrained to the upper limit of its deadband. Because of the randomization step, a load may become stuck at a high temperature, thus preventing it from providing sustained flexibility throughout the time horizon. Figure 2b presents a load that, when lock-out and deadband constraints permit, is frequently dispatched to follow the set-point, sometimes providing an increase in power consumption continuously over several rounds.

Figure 3 shows the regret for bOGD with and without randomization (relaxed decisions), averaged over 100 randomization steps ($\langle bOGD \rangle$), and its regret bound. The averaged regret approximates the expected regret. Figure 3 shows that in the current setting the regret (i) outperforms the bound provided in Theorem 1, (ii) is sublinear, thus showing that the decisions made with bOGD are approaching the round optimum at t increases, and (iii) is similar to the regret without randomization and averaged over several simulations.

V. CONCLUSION

In this paper, motivated by real-world demand response constraints, we incorporate binary constraints into OCO. We show that the expected dynamic regret of bOGD is sublinear in the time horizon and linear in the cumulative variation in round optima. We use bOGD for real-time DR with TCLs. We model the discrete on/off settings of the cooling units

and unavailability due to lock-out, temperature deadbands, and manual override.

Numerical simulations show that the randomization step yields a 1.34% deviation, on average, from the relaxed decisions. The relative tracking error is 6.91% and 6.92%, respectively, for the binary and relaxed algorithms. The algorithm is easy to implement and does not need extensive monitoring, data, or models. On average, less than 0.1 second is required to compute decisions for 1000 loads.

APPENDIX

A. Proof of Lemma 1

The Lipschitz continuity of f_t with respect to $\|\cdot\|_2$ yields

$$\mathbb{E} [|f_t(\hat{\mathbf{x}}_t) - f_t(\mathbf{x}_t)|] \leq \mathbb{E} [L_2 \|\hat{\mathbf{x}}_t - \mathbf{x}_t\|_2].$$

We rearrange the right-hand side to obtain

$$\begin{aligned} \mathbb{E} [|f_t(\hat{\mathbf{x}}_t) - f_t(\mathbf{x}_t)|] &\leq L_2 \mathbb{E} \left[\sqrt{\sum_{i=1}^n (\hat{\mathbf{x}}_t(i) - \mathbf{x}_t(i))^2} \right] \\ &\leq L_2 \sqrt{\sum_{i=1}^n \mathbb{E} [(\hat{\mathbf{x}}_t(i) - \mathbf{x}_t(i))^2]}, \end{aligned} \quad (7)$$

where we have used Jensen's inequality for concave function to obtain the second inequality. By definition of the randomization function, we have $\mathbb{E}[\hat{\mathbf{x}}_t] = \mathbf{x}_t$ and thus (7) can be re-expressed as:

$$\mathbb{E} [|f_t(\hat{\mathbf{x}}_t) - f_t(\mathbf{x}_t)|] \leq L_2 \sqrt{\sum_{i=1}^n \mathbb{E} [(\hat{\mathbf{x}}_t(i) - \mathbb{E}[\hat{\mathbf{x}}_t(i)])^2]}.$$

The expectation now represents the variance. Re-expressing the variance in terms of the first and second moment leads to

$$\mathbb{E} [|f_t(\hat{\mathbf{x}}_t) - f_t(\mathbf{x}_t)|] \leq L_2 \sqrt{\sum_{i=1}^n \mathbb{E} [\hat{\mathbf{x}}_t(i)^2] - \mathbb{E} [\hat{\mathbf{x}}_t(i)]^2}.$$

We have $\mathbb{E}[\hat{\mathbf{x}}_t(i)^2] = \mathbf{x}_t(i)$ and $\mathbb{E}[\hat{\mathbf{x}}_t(i)]^2 = \mathbf{x}_t(i)^2$ which follows from the definition of \mathcal{R} . Hence, we obtain

$$\mathbb{E} [|f_t(\hat{\mathbf{x}}_t) - f_t(\mathbf{x}_t)|] \leq L_2 \sqrt{\sum_{i=1}^n \mathbf{x}_t(i) - \mathbf{x}_t(i)^2}.$$

The variable $\mathbf{x}_t(i) \geq 0$ and thus

$$\begin{aligned} \mathbb{E} [|f_t(\hat{\mathbf{x}}_t) - f_t(\mathbf{x}_t)|] &\leq L_2 \sqrt{\sum_{i=1}^n \mathbf{x}_t(i)} \\ &= L_2 \sqrt{\sum_{i=1}^n |\mathbf{x}_t(i)|} \\ &= L_2 \sqrt{\|\mathbf{x}_t\|_1}. \end{aligned} \quad (8)$$

Let

$$\mathbf{y}_t = \arg \min_{\mathbf{x} \in \mathcal{X}} \eta \nabla f_{t-1}(\mathbf{x}_{t-1})^\top \mathbf{x} + \frac{1}{2} \|\mathbf{x} - \mathbf{x}_{t-1}\|_2^2, \quad (9)$$

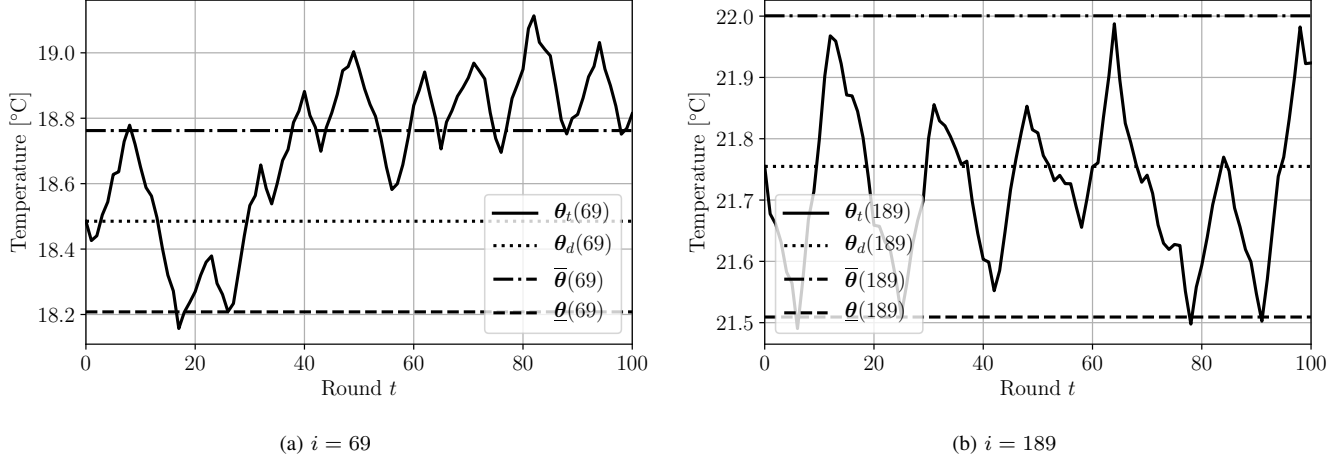


Fig. 2. Temperature profile of two selected TCLs during DR

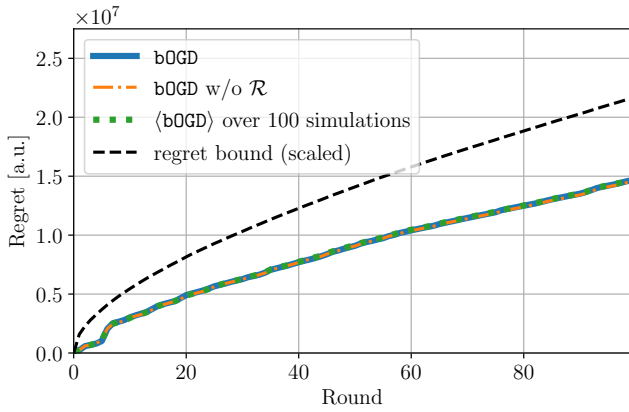


Fig. 3. Regret comparison of bOGD

and recall

$$\mathbf{x}_t = \arg \min_{\mathbf{x} \in \mathcal{X}} \eta \nabla f_{t-1}(\mathbf{x}_{t-1})^\top \mathbf{x} + \frac{1}{2} \|\mathbf{x} - \mathbf{x}_{t-1}\|_2^2 + \eta \lambda \|\mathbf{x}\|_1.$$

Thus, we have $\|\mathbf{x}_t\|_1 \leq \|\mathbf{y}_t\|_1$ which holds with equality for $\lambda = 0$ because the definitions of \mathbf{y}_t and \mathbf{x}_t differ only in the last term. Equation (9) is equivalent to the standard online gradient descent (OGD) update, i.e., a projected gradient step (with respect to the Euclidian norm). To show this, we start from the projected gradient step and expand the argument of the projection. Let $\mathcal{P} = \text{proj}_{\mathcal{X}}(\mathbf{x}_{t-1} - \eta \nabla f_{t-1}(\mathbf{x}_{t-1}))$. We have

$$\begin{aligned} \mathcal{P} &= \arg \min_{\mathbf{x} \in \mathcal{X}} \frac{1}{2} \|\mathbf{x} - (\mathbf{x}_{t-1} - \eta \nabla f_{t-1}(\mathbf{x}_{t-1}))\|_2^2 \\ &= \arg \min_{\mathbf{x} \in \mathcal{X}} \eta \nabla f_{t-1}(\mathbf{x}_{t-1})^\top \mathbf{x} - \eta \nabla f_{t-1}(\mathbf{x}_{t-1})^\top \mathbf{x}_{t-1} \\ &\quad + \frac{\eta^2}{2} \|\nabla f_{t-1}(\mathbf{x}_{t-1})\|_2^2 + \frac{1}{2} \|\mathbf{x} - \mathbf{x}_{t-1}\|_2^2 \\ &= \arg \min_{\mathbf{x} \in \mathcal{X}} \eta \nabla f_{t-1}(\mathbf{x}_{t-1})^\top \mathbf{x} + \frac{1}{2} \|\mathbf{x} - \mathbf{x}_{t-1}\|_2^2, \end{aligned}$$

where the last equation holds because $-\eta \nabla f_{t-1}(\mathbf{x}_{t-1})^\top \mathbf{x}_{t-1} + \frac{\eta^2}{2} \|\nabla f_{t-1}(\mathbf{x}_{t-1})\|_2^2$ do not depend on \mathbf{x} . From the property

of projections and the triangle inequality [1], we have

$$\|\mathbf{y}_t\|_1 \leq \|\mathbf{x}_{t-1} - \eta \nabla f_{t-1}(\mathbf{x}_{t-1})\|_1,$$

and hence

$$\|\mathbf{x}_t\|_1 \leq \|\mathbf{x}_{t-1} - \eta \nabla f_{t-1}(\mathbf{x}_{t-1})\|_1. \quad (10)$$

We further bound the right-hand side of (10) to obtain:

$$\begin{aligned} \|\mathbf{x}_t\|_1 &\leq \|\mathbf{x}_{t-1}\|_1 + \eta \|\nabla f_{t-1}(\mathbf{x}_{t-1})\|_1 \\ &\leq n + \eta L_1 \\ &\leq \eta L_1 (n + 1), \end{aligned} \quad (11)$$

because $\eta L_1 \geq 1$ by assumption. Substituting (11) into (8) leads to

$$\begin{aligned} \mathbb{E} [|f_t(\hat{\mathbf{x}}_t) - f_t(\mathbf{x}_t)|] &\leq L_2 \sqrt{\eta L_1 (n + 1)} \\ &\leq \eta L_1 L_2 \sqrt{n + 1}, \end{aligned}$$

where we have use the fact that $\eta L_1 \geq 1$ again. \square

B. Proof of Lemma 2

The expected regret of bOGD is

$$\mathbb{E} [\mathbb{R}_T] = \mathbb{E} \left[\sum_{t=1}^T f_t(\hat{\mathbf{x}}_t) - f_t(\mathbf{b}_t^*) \right],$$

where we recall that $\mathbf{b}_t^* \in \arg \min_{\mathbf{x}_t \in \{0,1\}^n} f_t(\mathbf{x}_t)$, an exact optimum. We can bound above the right-hand side by

$$\mathbb{E} [\mathbb{R}_T] \leq \mathbb{E} \left[\sum_{t=1}^T f_t(\hat{\mathbf{x}}_t) - f_t(\mathbf{x}_t^*) \right],$$

because \mathbf{x}_t^* is a relaxed optimum and $f_t(\mathbf{x}_t^*) \leq f_t(\mathbf{b}_t^*)$. Rearranging the terms, we obtain

$$\begin{aligned} \mathbb{E} [\mathbb{R}_T] &= \sum_{t=1}^T \mathbb{E} [f_t(\hat{\mathbf{x}}_t) + f_t(\mathbf{x}_t) - f_t(\mathbf{x}_t) - f_t(\mathbf{x}_t^*)] \\ &\leq \sum_{t=1}^T \mathbb{E} [|f_t(\hat{\mathbf{x}}_t) - f_t(\mathbf{x}_t)|] + f_t(\mathbf{x}_t) - f_t(\mathbf{x}_t^*) \\ &= \mathbb{R}_T (\text{OGD-R}_1) + \sum_{t=1}^T \mathbb{E} [|f_t(\hat{\mathbf{x}}_t) - f_t(\mathbf{x}_t)|], \end{aligned}$$

where $R_T(\text{OGD-R}_1)$ denotes the regret of the standard OGD algorithm with ℓ_1 -regularization [24]. Using Lemma 1 yields

$$\mathbb{E}[R_T] \leq R_T(\text{OGD-R}_1) + \sum_{t=1}^T \eta L_1 L_2 \sqrt{n+1}. \quad (12)$$

By [24, Theorem 2] with $\Phi_t = \mathbf{I}$, $\psi(\mathbf{x}) = \frac{1}{2} \|\mathbf{x}\|_2^2$, and $r(\mathbf{x}) = \lambda \|\mathbf{x}\|$, we upper bound the regret of OGD-R₁:

$$R_T(\text{OGD-R}_1) \leq \frac{D_{\max}}{\eta} + \frac{2L_\psi}{\eta} V_T + \frac{(L_2)^2 \eta T}{2\sigma},$$

where $D_{\max} = \frac{n}{2} \geq \frac{1}{2} \|\mathbf{x} - \mathbf{y}\|_2^2$ (the Bregman divergence with respect to ψ) for all $\mathbf{x}, \mathbf{y} \in \mathcal{X}$, $L_\psi = n$ is a Lipschitz constant for $\frac{1}{2} \|\mathbf{x} - \mathbf{y}\|_2^2$ and $\sigma = 1$, the strong-convexity modulus of ψ . We then have

$$R_T(\text{OGD-R}_1) \leq \frac{n}{2\eta} + \frac{2n}{\eta} V_T + \frac{(L_2)^2 \eta T}{2}. \quad (13)$$

We upper bound (12) using (13) and obtain

$$\begin{aligned} \mathbb{E}[R_T] &\leq \frac{n}{2\eta} + \frac{2n}{\eta} V_T + \frac{(L_2)^2 \eta T}{2} + \sum_{t=1}^T \eta L_1 L_2 \sqrt{n+1} \\ &= \frac{n}{2\eta} + \frac{2nL_1}{\eta L_1} V_T + \frac{(L_2)^2 \eta T}{2} + \eta L_1 L_2 T, \end{aligned}$$

where we have multiplied the second term by L_1/L_1 . By assumption, $\eta L_1 \geq 1$ and hence

$$\mathbb{E}[R_T] \leq \frac{n}{2\eta} + 2nL_1 V_T + \frac{(L_2)^2 \eta T}{2} + \eta L_1 L_2 T.$$

Setting $\eta = \frac{a}{\sqrt{T}}$ completes the proof. \square

REFERENCES

- [1] E. Hazan *et al.*, “Introduction to online convex optimization,” *Foundations and Trends® in Optimization*, vol. 2, no. 3-4, pp. 157–325, 2016.
- [2] S. Shalev-Shwartz *et al.*, “Online learning and online convex optimization,” *Foundations and Trends® in Machine Learning*, vol. 4, no. 2, pp. 107–194, 2012.
- [3] S.-J. Kim and G. B. Giannakis, “An online convex optimization approach to real-time energy pricing for demand response,” *IEEE Transactions on Smart Grid*, vol. 8, no. 6, pp. 2784–2793, 2016.
- [4] A. Lesage-Landry and J. A. Taylor, “Setpoint tracking with partially observed loads,” *IEEE Transactions on Power Systems*, vol. 33, no. 5, pp. 5615–5627, 2018.
- [5] D. S. Callaway, “Tapping the energy storage potential in electric loads to deliver load following and regulation, with application to wind energy,” *Energy Conversion and Management*, vol. 50, no. 5, pp. 1389–1400, 2009.
- [6] J. L. Mathieu, S. Koch, and D. S. Callaway, “State estimation and control of electric loads to manage real-time energy imbalance,” *IEEE Transactions on Power Systems*, vol. 28, no. 1, pp. 430–440, 2012.
- [7] H. Hao, Y. Lin, A. S. Kowli, P. Barooah, and S. Meyn, “Ancillary service to the grid through control of fans in commercial building hvac systems,” *IEEE Transactions on smart grid*, vol. 5, no. 4, pp. 2066–2074, 2014.
- [8] D. S. Callaway and I. A. Hiskens, “Achieving controllability of electric loads,” *Proceedings of the IEEE*, vol. 99, no. 1, pp. 184–199, 2010.
- [9] J. A. Taylor, S. V. Dhople, and D. S. Callaway, “Power systems without fuel,” *Renewable and Sustainable Energy Reviews*, vol. 57, pp. 1322–1336, 2016.
- [10] F. S. Hillier and G. J. Lieberman, *Introduction to operations research*. McGraw-Hill Science, Engineering & Mathematics, 1995.
- [11] E. Hazan and S. Kale, “Online submodular minimization,” *Journal of Machine Learning Research*, vol. 13, no. Oct, pp. 2903–2922, 2012.
- [12] S. Jegelka and J. A. Bilmes, “Online submodular minimization for combinatorial structures.” in *ICML*. Citeseer, 2011, pp. 345–352.
- [13] A. R. Cardoso and R. Cummings, “Differentially private online submodular minimization,” in *The 22nd International Conference on Artificial Intelligence and Statistics*, 2019, pp. 1650–1658.
- [14] F. Bach, “Submodular functions: from discrete to continuous domains,” *Mathematical Programming*, vol. 175, no. 1-2, pp. 419–459, 2019.
- [15] S. Iwata, L. Fleischer, and S. Fujishige, “A combinatorial strongly polynomial algorithm for minimizing submodular functions,” *Journal of the ACM (JACM)*, vol. 48, no. 4, pp. 761–777, 2001.
- [16] L. Lovász, “Submodular functions and convexity,” in *Mathematical Programming The State of the Art*. Springer, 1983, pp. 235–257.
- [17] S. Bubeck, “Introduction to online optimization,” 2011. [Online]. Available: <http://sbubeck.com/BubeckLectureNotes.pdf>
- [18] J.-Y. Audibert, S. Bubeck, and G. Lugosi, “Regret in online combinatorial optimization,” *Mathematics of Operations Research*, vol. 39, no. 1, pp. 31–45, 2014.
- [19] X. Zhou, E. Dall’Anese, and L. Chen, “Online stochastic optimization of networked distributed energy resources,” *IEEE Transactions on Automatic Control*, 2019.
- [20] A. Bernstein and E. Dall’Anese, “Real-time feedback-based optimization of distribution grids: A unified approach,” *IEEE Transactions on Control of Network Systems*, vol. 6, no. 3, pp. 1197–1209, 2019.
- [21] A. Bernstein, N. J. Bouman, and J.-Y. L. Boudec, “Real-time minimization of average error in the presence of uncertainty and convexification of feasible sets,” *arXiv preprint arXiv:1612.07287*, 2016.
- [22] J.-B. Hiriart-Urruty and C. Lemaréchal, *Convex analysis and minimization algorithms I: Fundamentals*. Springer science & business media, 2013, vol. 305.
- [23] M. Zinkevich, “Online convex programming and generalized infinitesimal gradient ascent,” in *Proceedings of the 20th International Conference on Machine Learning (ICML-03)*, 2003, pp. 928–936.
- [24] E. C. Hall and R. M. Willett, “Online convex optimization in dynamic environments,” *IEEE Journal of Selected Topics in Signal Processing*, vol. 9, no. 4, pp. 647–662, 2015.
- [25] A. Mokhtari, S. Shahrampour, A. Jadbabaie, and A. Ribeiro, “Online optimization in dynamic environments: Improved regret rates for strongly convex problems,” in *2016 IEEE 55th Conference on Decision and Control (CDC)*, 2016, pp. 7195–7201.
- [26] J. C. Duchi, S. Shalev-Shwartz, Y. Singer, and A. Tewari, “Composite objective mirror descent.” in *COLT*, 2010, pp. 14–26.
- [27] J. L. Mathieu, M. Kamgarpour, J. Lygeros, G. Andersson, and D. S. Callaway, “Arbitraging intraday wholesale energy market prices with aggregations of thermostatic loads,” *IEEE Transactions on Power Systems*, vol. 30, no. 2, pp. 763–772, 2015.
- [28] V. C. Gungor, D. Sahin, T. Kocak, S. Ergut, C. Buccella, C. Cecati, and G. P. Hancke, “A survey on smart grid potential applications and communication requirements,” *IEEE Transactions on industrial informatics*, vol. 9, no. 1, pp. 28–42, 2012.
- [29] S. Diamond and S. Boyd, “CVXPY: A Python-embedded modeling language for convex optimization,” *Journal of Machine Learning Research*, vol. 17, no. 83, pp. 1–5, 2016.
- [30] Gurobi Optimization, Inc., “Gurobi optimizer reference manual,” 2016. [Online]. Available: <http://www.gurobi.com>